INTEGRATION OF DIGITAL PHOTOGRAMMETRY AND CAAD: CONSTRAINT-BASED MODELLING AND SEMI-AUTOMATIC MEASUREMENT

André Streilein
Institute of Geodesy and Photogrammetry
Swiss Federal Institute of Technology Zurich
CH-8093 Zurich
e-mail: andre@p.igp.ethz.ch

Urs Hirschberg
Chair of Architecture and CAAD
Swiss Federal Institute of Technology Zurich
CH-8093 Zurich
e-mail: hirsch@arch.ethz.ch

ABSTRACT

The integration of state-of-the-art photogrammetric methods with the capabilities of CAAD has great potential for a variety of architectural applications. This paper describes the current status of an ongoing research project which aims to develop an easy to use tool for the photogrammetric generation of accurate, reliable and well structured 3D CAAD models of architectural objects.

The system essentially consists of a standard CAAD package to which additional functionality was added and a Digital Photogrammetry Station (DIPS), providing semi-automatic computer measurement. The paper concentrates on two main issues in the design of the system: the data-integration and the caad-based 3D feature extraction. The data-integration is achieved using a knowledge-base. On top of an adequate data-transfer between the two systems this knowledge-base enables constraint-based modelling in CAAD and qualitatively controlled measurement in DIPS. In the section about Digital Photogrammetry we describe the 3D feature extraction procedure in detail and point out how the qualitative control can be achieved. A practical example is used to illustrate the performance of the system.

1. INTRODUCTION

Nowadays surveying methods based on imaging sensors are used in many applications in computer vision, robotics, machine vision and industrial metrology. The hardware for these applications with powerful workstations and digital imaging sensors has become available and affordable over the past few years. As photogrammetry basically means measuring in image, a system for digital photogrammetry must necessarily be a hybrid, processing both image and vector data. This hybrid functionality can be employed in a great variety of applications. In monument preservation or archaeology it can be used to produce very detailed documentations in plans, images and database-records. In urban planning images can be interpreted in a much less detailed way to produce abstract yet correct and reliable 3D models of “city-scapes” useful as references to judge new projects. In some applications the production of traditional architectural as-built plans will be most important, such as for renovations or alterations of existing buildings for which no or only inaccurate plans exist. In the growing field of virtual reality on the other hand, the production of rectified texturemaps from perspective images is another application. It is important to mention this variety of uses, not only to show that digital photogrammetry is an interesting topic for

Presented paper on the CAAD Futures ‘95 International Conference, 24-26 September 1995, Singapore

CAAD, but also to explain why we pursued openness and general applicability as two of the key aspects in the design of our system.

A number of commercial software packages useful for architectural photogrammetry are available on the market [1] [2]. As they are restricted to manual measurements, the accuracy of the delivered data is highly dependent on the dexterity of the operator. On top of that the application of these programs is usually quite time-intensive and requires special training. These shortcomings may account for the fact that these methods are still rather rarely made use of in the architectural practice.

The system currently under development at the Swiss Federal Institute of Technology aims to overcome these shortcomings. It is a fully digital system for architectural photogrammetry not only in the sense that it transfers traditional photogrammetric techniques which usually involved very expensive mechanical equipment to a computer-terminal (which is, essentially, what the mentioned commercial packages do). Most importantly it takes advantage of the digital format of the data to increasingly automatize the time-consuming measurement process. These new semi-automatic measurement techniques create a need for a modelling strategy quite different from the one found in current CAAD systems. These special requirements are met making use of a knowledge-base which enables constraint-based modelling in CAAD as well as qualitative control in the photogrammetric 3D feature extraction.

2. SYSTEM OVERVIEW

The system combines digital photogrammetric methods with the capabilities of CAAD. The photogrammetric processing is performed with a Digital Photogrammetry Station (DIPS), while the architectural processing takes place in a CAAD environment. By customizing the functionality of an existing software package with a true programming interface (AutoCAD) we achieved an increasing integration of CAAD and DIPS in the course of the project. Presently the integration of the datastructures and the consistency of the user interface has reached a degree of completeness to make it reasonable to refer to the system as one entire whole: DIPAD (Digital System for Photogrammetry and Architectural Design) (see Figure 1).

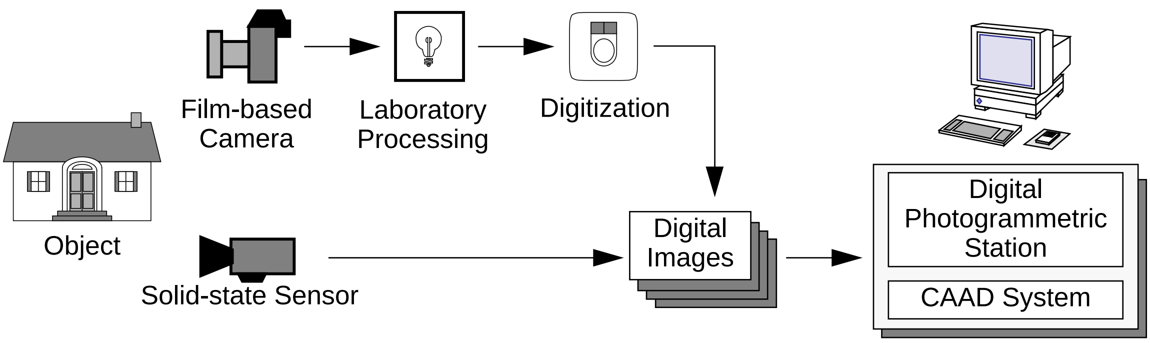

Figure 1: Digital Architectural Photogrammetry with DIPAD.

2.1. Image Acquisition

The image acquisition can be done with solid-state sensors or with film-based cameras and subsequent digitization. Today a variety of solid-state imaging systems are available on the market. For the application in architectural photogrammetry different requirements are of importance, e.g. high-resolution to image small object features, portability, high dynamic range to image large variations in scene brightness common to outdoor scenes, the ability to store a huge amount of image data and the metric accuracy performance. While traditional film-based cameras still provide unsurpassed image resolution, today's solid state sensors offer a number of advantages (on-site quality control, no subsequent digitization, low cost, etc.). An overview of existing systems for digital image acquisition is given in [3] [4].

2.2. Image Understanding: Interpreting Architecture

The main principle of DIPAD is that the human operator assumes responsibility of the image understanding part, while the actual measurement is automatically handled by the computer. The user indicates relevant parts of the object by approximating a geometric topology to it. The photogrammetric algorithm matches this topology with the image data of multiple images, thereby deriving its exact three dimensional position and geometry. This top-down strategy provides for high precision as well as for reliability. It is also quite straightforward as interpreting a scene is something very natural for humans and - as the computer vision community knows - very difficult for computers [5][6]. But this is not the reason why we adopted our semi-automatic strategy which lets the computer as well as the human operator each do what they are best at. We do pursue increasing automation in the long run! However, it is necessary to keep in mind what automation of an interpretative process means. In the case of architecture not the least of problems that this interpretative process faces is that there are no accepted rules that could govern it. Interpreting architecture is by no means a well-defined task. One does not have to go to the more academic considerations Venturi [7] or Slutzky and Rowe [8] point out. The problem arises at a much more fundamental level. There are no consistent theoretical suppositions underlying CAAD systems [9]. While there are many accepted ways to structure a model and even some standards as far as the use of layers goes, there are hardly two CAAD operators that would build the same model in the same way. For good reasons. There are many tricks and techniques experienced CAAD operators know about that come into play depending on the sorts of tasks a model will be used for. Whether it is used for the production of plans only, whether it will be used for rendering later, whether it is necessary to disintegrate the model in certain analytical ways to show a design intent, or whether texture maps are to be applied in a rendering system - usually all of these considerations evoke a different approach by the CAAD operator. And then much of it is personal style. So apart from the fact that it is simply difficult to automatically detect features, full automation of the interpretation of architectural images faces many other challenges.

Our approach is therefore to provide a very general tool that allows for different user intents and styles in the modelling process. Automation could then come in as a computer learning mechanism, in a way that the operator can teach his individual modelling preferences to the system. Rather than trying to invent an arbitrary model structuring strategy that will fit all purposes as the basis for automation (it is highly questionable that such a universal strategy could indeed be found) we incorporate the accepted structuring means as options into our system. This was one of the main reasons for using a standard CAAD system as a platform for DIPAD.

2.3. Components of DIPAD

DIPAD essentially consists of two systems: the CAAD system supports architectural 2D and 3D modelling facilities, whereas DIPS provides for the semi-automatic measuring procedures based on digital imagery. Both systems have their own datastructures which have evolved to suit their tasks best. Not surprisingly, the structures of the two systems - although both fundamentally rely on points in 3D-space - don't match. So in order to map the data in one database onto the database of the other system, it is necessary to provide an interface to exchange data.

In an earlier phase of the project, the DXF standard was used for this purpose [10]. But this is not only a rather unwieldy format that makes any type of run-time exchange very hard to achieve. Using DXF also meant to limit the data-exchange to the specific idiosyncrasies of the CAAD system. So what could indeed be exchanged was so to speak the smallest common denominator of the requirements of both systems. For successful further development of the project it was necessary to find a way to let both systems share all the relevant information. To achieve this we have developed a knowledge-base which is capable to fill in the missing information during the data-transfer from one system to the other. So rather than eliminating information in the transfer, additional information required by the receiving system that is not found in the sending one is added with the knowledge-base (see Figure 2).

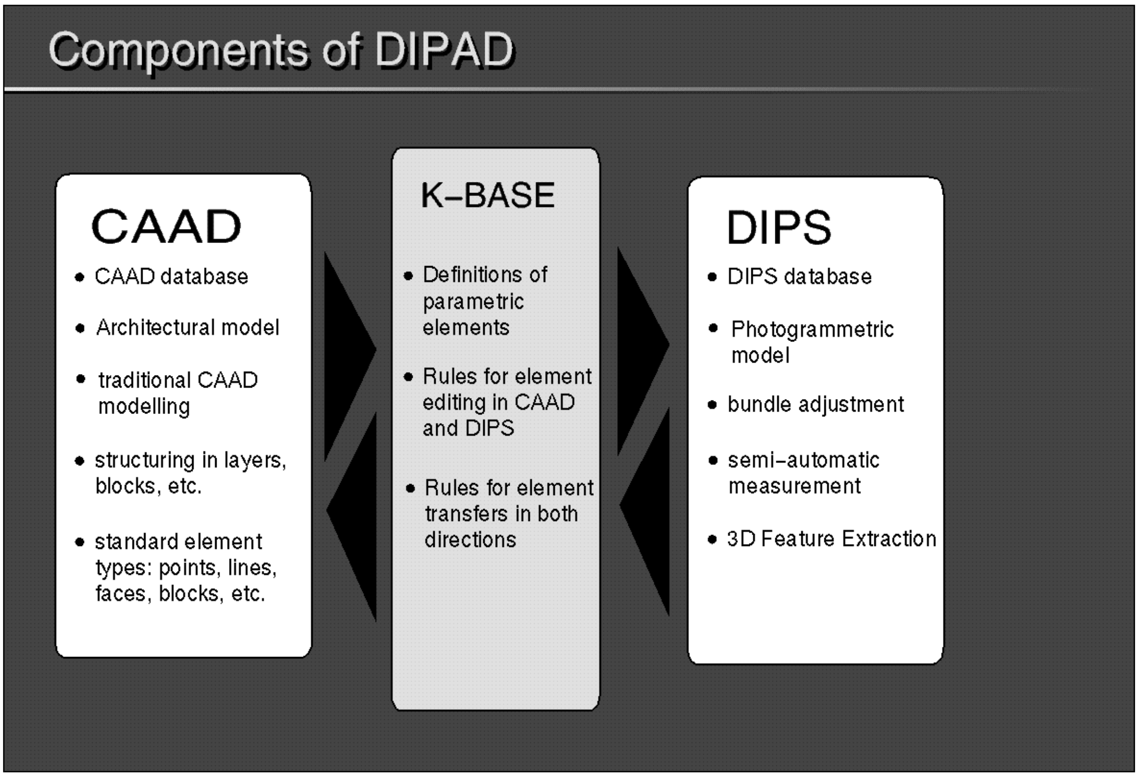

Figure 2: The knowledge-base enables the datamapping between DIPS and the CAAD and is used by both systems to supply constraints in the editing of elements.

Research into the use of knowledge-bases in design often focuses on semantic knowledge, probably because it is the most challenging from an AI standpoint [11]. So the term knowledge-base may be a bit misleading as our knowledge base does not provide or deal with any semantic knowledge at this point. It essentially holds the definitions of complex parametric objects as generative edgelists, facelists and parametric equations for every point. Though being a very simple and straightforward implementation of a knowledge-base, it allows that the elements can be constructed in the CAAD environment with traditional discrete elements and at the same time be evaluated as complex graphs with unique points in DIPS.

Data transfer is however only one of the possibilities that open up with the introduction of a knowledge-base that the two systems share. As we will point out in the next two sections it can also be used by both systems as guidance during the editing of objects.

3. MODELLING IN DIPAD

In the current version of DIPAD it is possible to perform all the editing on the model in the CAAD system while the objects are projected run-time into the previously oriented images. This means that DIPAD can make full use of the modelling capabilities of the CAAD program, getting instant feed-back about how closely the model matches the image. The photogrammetric measurement on the other side can include all the geometric and semantic information present in the CAAD system as constraints in the measurement process. Changes in the database of one system can be mapped onto the database of the other system instantly. So, modelling and measuring are smoothly integrated actions in one continuous work-flow (see Figure 3). All the procedures, the modelling as well as the transferring make use of the knowledge-base.

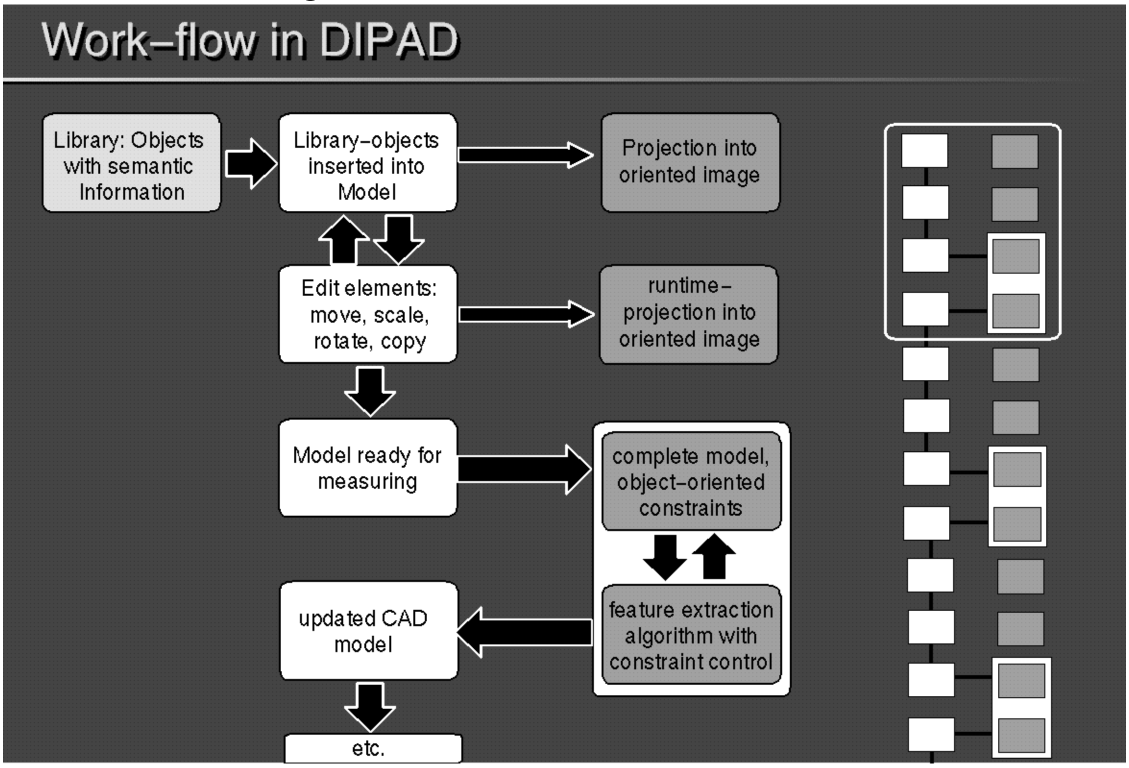

Figure 3: CAAD and Photogrammetry systems communicate runtime: modelling and measuring are smoothly integrated actions in one continous work-flow.

3.1. Controlling hybrid viewers from CAAD

Some of these functionalities are of quite general usefulness for architectural modelling. The little camera-icons in the CAAD system (see Figure 4) are linked with corresponding camera parameters of an image viewer. When the parameters of a camera-icon are edited in the CAAD system, the changes of its view can be entirely monitored in the viewer. This is primarily intended to facilitate the initial positioning of a camera with respect to the model (further refinement of the camera parameters is then done as part of the computer measurement). Moving around these icons can however also be used to do real-time fly-throughs in the model. This is quite effective especially because the analytical view of the model with the cameraposition is always visible concurrently. As the exact exterior orientation of an image is determined by DIPS, it is also possible to set up the exactly corresponding perspective in the CAAD system. This greatly facilitates the production of montages. So the functions we are developing are not only relevant in creating a precise model of an existing building, they also serve well when creating new buildings in existing contexts or even as general feedback generators during modelling.

Figure 4: The modelling in the CAAD system can be entirely monitored in the DIPAD viewer linked to the model. Each camera icon corresponds to one viewer.

3.2. Constraint-based Modelling

While all the accepted means of structuring a CAAD model (layers, blocks, level of detail) are well applicable within DIPAD, the form of the models that are the basis for the computer measuring must be defined qualitatively rather than quantitatively. We have described this qualitative or constraint-based modelling in more detail in [12], paraphrasing it as modelling “weak forms” or “objects with controllable deformability”. We also pointed out that this weak form quality offers a means to introduce a certain indeterminacy into CAAD modelling. This is essential in a model that is the basis for computer measurement, but also quite useful for designing with the computer in general.

Here we want to focus on the role of the knowledge-base as the facility that provides constraints for the CAAD modelling as well as the photogrammetric measurement. In CAAD, a set of functions that query the knowledge-base for these constraints support complete rubberbanding functionality for complex parametric objects. They have been implemented making intensive use of AutoCAD’s extended entity data (EED), a facility that allows storing of additional data with the entity data of an object. When such a parametric object is generated or edited, its name and current parameters are stored in EED. The name serves as a reference to the knowledge-base. In the knowledge-base for every element a variety of information, most importantly a sort of genetic code, that is its description in terms of points, lines, faces and parametric equations, is described. To edit these objects, special functions allow direct graphical interaction with all the specified parameters. They can, however, be edited with the standard AutoCAD commands as well. They behave like standard blocks in that case. These objects are available in a library. With the special functions, their insertion and editing can be entirely monitored in the external viewers. So even during the interaction with the model all changes become visible as projections overlaid on the actual image of the architectural object that is to be modelled and measured. As approximations to the actual positions are sufficient, this modelling is very intuitive and fast.

The parametrization of the individual objects is what we call internal constraints. In much the same way as internal constraints we plan to implement what we refer to as external constraints. Formulating external constraints means that constrained relationships between different objects, can be introduced by attaching or nesting the individual (parametric) objects to one another. Both methods, nesting as well as attaching, define a fixed geometric relationship between two objects: they can share an edge, have complanar sides or the like. Nesting an element also introduces a hierarchy in the model which can be used as a means to provide different levels of detail.

The main raison d'être of the constraint-based modelling is the transfer of architectural information to DIPS. The constraints contained in the knowledge-base can be included as so-called observations in the bundle adjustment, which is described in the next section. In this way they provide qualitative guidance in the photogrammetric measurement. Without any qualitative guidance the accuracy of the measuring process creates unwanted results. For example four points that “obviously” lie on one plane (maybe the corners of a door) will be slightly offset. This creates unnecessarily complex and irregular models, even if the measurement actually reflects the physical condition of that particular door correctly. The user gets feed-back about the reliability of the extracted features by the underlying stochastic model. It is then possible to either select a different parametric object or to increase the level of tolerance. This way a user is always informed about the correctness of their assumptions as well as the precision of the model that is generated.

4. DIGITAL PHOTOGRAMMETRY - 3D FEATURE EXTRACTION

The task of converting an iconic representation of an object (raster image, unstructured information) into a symbolic representation (vector an attribute data in structured form) with high accuracy is solved within DPAD by a three-dimensional feature extraction routine (3D-FEX). It is a semi-automatic routine, where a series of model- and data-driven processes interact to extract geometric information from the digital imagery. A generic semantic object model is used to detect the features described by this model. Therefore, only relevant features (as defined by the user) are extracted and redundant or useless informations are reduced to a minimum. In addition, the use of a priori knowledge makes explicit assumptions, that allows the checking of whether or not these assumptions are fulfilled in the images (e.g. constraints from the knowledge-base). In addition this approach acts rather globally, which means that small deformations (e.g. image noise, blurred image structures, etc.) in general do not effect the estimated result.

The three-dimensional position of the object is derived by a simultaneous multi-frame feature extraction, where the object model is reconstructed and used to triangulate the object points from corresponding image points.

Looking at images taken for architectural photogrammetry it is evident that in the most cases linear boundaries (edges) of an architectural feature contain more information than the vertices (corners) of this feature. Although edges are only a small percentage of the whole image content, they have major importance for the description of object discontinuities. The 3D-FEX routine takes advantage of this knowledge, by first locating the edges of the features to be measured and then deriving the vertices as intersections of appropriate lines. This routine consists basically of three loops. First an internal loop performs the feature extraction in 2D-space, based on the radiometric information given by the digital imagery. An external loop allows the robust determination of object coordinates from multi-frames, and finally an orientation loop provides for the estimation of camera parameters (interior/exterior orientation) by a bundle adjustment, which is necessary as these are a priori unknowns.

4.1. Internal loop

The approximation of generic object space features transformed into image space are used as starting values for the two-dimensional automatic extraction algorithm. This algorithm is based on the assumption that discontinuities or rapid changes in the intensity of the image signal often occur at the physical extent (edges) of objects within the image. The localization of an edge in image domain is equivalent to finding the maximum of the first partial derivatives (gradients) of the image intensity function.

In a continuous domain f(x,y) an edge can be detected by forming a continuous one-dimensional gradient g(x,y) along a line normal to the edge slope, which is at an angle θ with respect to the horizontal axis. The gradient along the line normal to the edge slope can be computed in terms of derivatives along the orthogonal axis (Eq. 1).

$$g(x, y) = \frac{\partial f(x, y)}{\partial x} \cdot \cos\theta + \frac{\partial f(x, y)}{\partial y} \cdot \sin\theta \qquad \text{(Eq. 1)}$$

The edge gradient g(j,k) in the discrete spatial domain f(j,k) (e.g. image intensity function) is described in terms of a row gradient $g_r(j,k)$ and a column gradient $g_c(j,k)$. The row and column gradients are computed by the convolution relationship:

$$\begin{aligned} g_r(j, k) &= f(j, k) \otimes h_r(j, k) = \sum\sum f(m, n) \cdot h_r(m - j - d, n - k + d) \\ g_c(j, k) &= f(j, k) \otimes h_r(j, k) = \sum\sum f(m, n) \cdot h_r(m - j - d, n - k + d) \end{aligned} \qquad \text{(Eq. 2)}$$

where $h_r(j,k)$ and $h_c(j,k)$ are the l by l impulse response arrays, with d = (l+1)/2.

The simplest method of discrete gradient generation is to form the running differences along rows and columns of the image. Commonly used operators for discrete gradient generation use a smoothing operator in combination with a differencing operator. The Sobel operator (as used in 3D-FEX) concatenates three binomial filters for smoothing (Eq. 3).

$$h_r = \frac{1}{8}\begin{bmatrix} 1 & 2 & 1 \\ 0 & 0 & 0 \\ -1 & -2 & -1 \end{bmatrix}, \qquad h_c = \frac{1}{8}\begin{bmatrix} 1 & 0 & -1 \\ 2 & 0 & -2 \\ 1 & 0 & -1 \end{bmatrix} \qquad \text{(Eq. 3)}$$

The spatial gradient amplitude is given by:

$$g(j, k) = \sqrt{g_r(j, k)^2 + g_c(j, k)^2} \qquad \text{(Eq. 4)}$$

The direction of the spatial gradient with respect to the row axis is:

$$\theta(j, k) = \arctan\frac{g_c(j, k)}{g_r(j, k)} \qquad \text{with } -\pi < \theta < \pi \qquad \text{(Eq. 5)}$$

Every pixel is assigned a gradient value, which is a vector containing the amplitude and the direction. The position of the edge is then determined with subpixel precision by fitting a second-order polynomial in the direction of the gradient. The maximum point of the fitting curve corresponds to the subpixel position of the edge (see Figure 5).

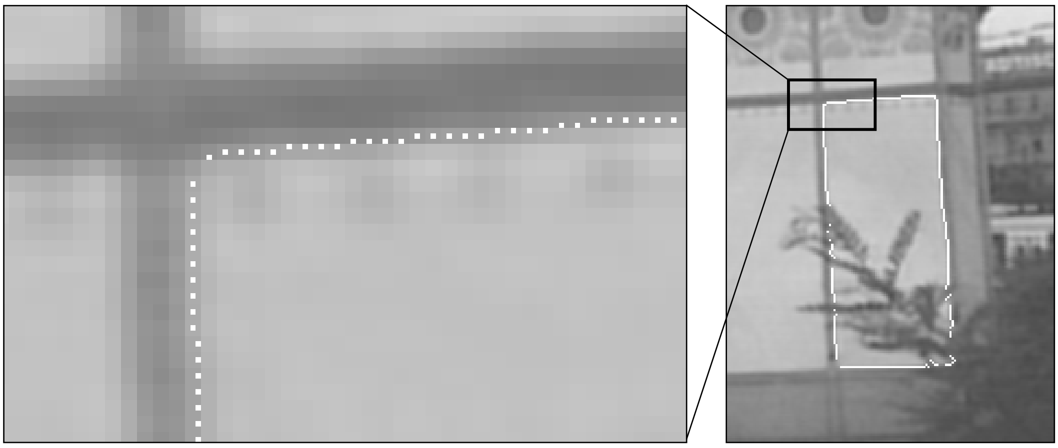

Figure 5: Zoom of extracted image edge points (sub-pixel precision).

The boundary elements of all objects within the image will be detected, and the algorithm converts this raster data into vector format by fitting straight lines to the linear boundaries. These vectors will then be used to determine the image coordinates of object vertices by line intersection. The internal loop delivers image coordinates for the vertices of features with a precision of 0.2-0.02 pixel.

4.2. External loop and orientation loop

The internal loop is performed sequentially in all images. The object coordinates of a point imaged in two or more images are calculated either by a spatial intersection, by a bundle adjustment or by a bundle adjustment with self-calibration, depending on which model parameters are treated as a priori known or unknown. The derived object coordinates are then projected into each image and used to restart the internal loop.

All these tasks of calculating object coordinates from image coordinate observations are subtasks of the general problem of positioning, which can generally be defined to be the determination of the orientation elements of one or more cameras, the coordinates of object points, parameters of analytical object descriptions, and in case of calibration additional parameters [13]. The bundle method, established in the 1950’s by Brown [14] and Schmid [15], is used to solve the positioning problem. It is based on a mathematical camera model comprised of separate functional and stochastic models. The functional model describing the relationship between the derived and measured quantities consists of the well known collinearity equations. The collinearity equations (Eq. 6), derived from the perspective transformation, are based on the fundamental assumption that the perspective center, the ground point and its corresponding image point lie on a straight line. For each pair of image coordinates (x, y) observed on each image the following pair of equations is written:

$$F_x = (x - x_p) = -c\,\frac{U}{W}, \qquad F_y = (y - y_p) = -c\,\frac{V}{W} \qquad \text{(Eq. 6)}$$

with the auxiliaries:

$$\begin{bmatrix} U \\ V \\ W \end{bmatrix} = D(\omega, \varphi, \kappa) \begin{bmatrix} X - X_0 \\ Y - Y_0 \\ Z - Z_0 \end{bmatrix} \qquad \text{(Eq. 7)}$$

with the image coordinates (x, y), the elements of interior orientation (x_p, y_p, c), the object coordinates (X, Y, Z), a 3 by 3 orthogonal rotation matrix D with the three rotations ω, φ, κ and the object coordinates of the perspective centre (X_0, Y_0, Z_0). The elements of interior orientation (x_p, y_p, c) define the location of the centre of perspective in the image coordinate system (physically the front nodal point). The exterior orientation elements define the location of the perspective centre in object space and the orientation of the image coordinate system with respect to the object coordinate system.

In reality, image formation by optical sensors derivates from an ideal perspective transformation. Consequently, image coordinates observations contain systematic errors with respect to the functional model (Eq. 6). These are accounted for by extending the collinearity equations with functions of additional parameters:

$$F_x = (x - x_p) = -c\frac{U}{W} + \Delta x,\; F_y = (y - y_p) = -c\frac{V}{W} + \Delta y \qquad \text{(Eq. 8)}$$

with Δx and Δy as functions of the additional parameters.

Many additional parameter sets have been developed to meet various requirements. Some attempt to model the specific characteristics of systematic errors, e.g. distortion, others are designed to absorb any kind of deformation. The selection of a particular parameter set depends on the application and the accuracy requirements. In close-range photographic and CCD-sensor based systems the following set of additional parameters has proven to be effective [16][17]:

$$\begin{aligned} \Delta x &= \Delta x_p - \frac{\bar{x}}{c}\Delta c - \bar{x}\, s_x + \bar{y}\, a + \bar{x}r^2k_1 + \bar{x}r^4k_2 + \bar{x}r^6k_3 + \left(r^2 + 2\bar{x}^2\right)p_1 + 2\bar{x}\bar{y}p_2 \\ \Delta y &= \Delta y_p - \frac{\bar{y}}{c}\Delta c + \bar{x}\, a + \bar{y}r^2k_1 + \bar{y}r^4k_2 + \bar{y}r^6k_3 + 2\bar{x}\bar{y}p_1 + \left(r^2 + 2\bar{y}^2\right)p_2 \end{aligned} \qquad \text{(Eq. 9)}$$

with $\bar{x} = x - x_p$, $\bar{y} = y - y_p$ and $r^2 = \bar{x}^2 + \bar{y}^2$.

This equation is called a “physical model” because each of its components can be directly attributed to physical systematic error sources; i.e. Δx_p, Δy_p and Δc represents changes of the interior orientation elements, s_x represents the scale factor in x, a represents a shear factor, k_1, k_2, k_3 are the first three parameters of radial symmetric lens distortion, and p_1, p_2 are the first two parameters of lens decentering distortion.

The simultaneous estimation of all parameters of Eq. 8 by a least squares estimation is formulated in the Gauss-Markov model as:

$$E(y) = Ax = y + e \qquad \text{(Eq. 10)}$$

with $E(e) = 0$ and $D(e) = D(y) = \sigma_0^2 P^{-1} = \sigma_0^2 \Sigma_{yy}$

It relates the *n* expected values E(y) of the observations y (i.e. image coordinates) and the *u* unknown parameters x (depending on the task) in a linear manner. The coefficients (a_{ij}) of the design matrix A are derived from a linearization of the non-linear model E(y) = f(x), A then being the matrix of partial derivatives df_i/dx_j. The variance covariance matrix Σ of the observations is assumed to be known except for an unknown variance factor σ_0^2.

Starting from observed values y the overconstrained equation system (Eq. 10) can be solved leading to estimates x for the unknown parameters.

$$\hat{x} = (A^T P A)^{-1} \cdot A^T P y \qquad \text{(Eq. 11)}$$

With the estimates values of x we can derive the fitted values, which “fit” the model and are estimates of the expectation E(y). The differences ê are corrections of the observed values or the residuals. With them we can obtain an estimate for the variance factor $\sigma_0{}^2$.

$$\hat{\sigma}_0^2 = \frac{\hat{e}^T P \hat{e}}{r} = \frac{\hat{e}^T P \hat{e}}{n-u}, \qquad \text{with } \hat{e} = A\hat{x} - y = \hat{y} - y \qquad \text{(Eq. 12)}$$

Now the precision of the estimates x can be derived by error propagation.

$$\hat{D}(\hat{x}) = \Sigma_{\hat{x}\hat{x}} = \hat{\sigma}_0^2 \cdot Q_{\hat{x}\hat{x}} = \hat{\sigma}_0^2 \cdot \left(A^T P A\right)^{-1} \qquad \text{(Eq. 13)}$$

The standard deviations of object space coordinates are given by:

$$\hat{\sigma}_{X_i} = \hat{\sigma}_0 \sqrt{q_{X_i X_i}}, \qquad \hat{\sigma}_{Y_i} = \hat{\sigma}_0 \sqrt{q_{Y_i Y_i}}, \qquad \hat{\sigma}_{Z_i} = \hat{\sigma}_0 \sqrt{q_{Z_i Z_i}} \qquad \text{(Eq. 14)}$$

with $q_{X_i X_i}$ as the diagonal element of the inverse of the normal equation matrix at the position of the corresponding unknown.

(a.) part of a scene.

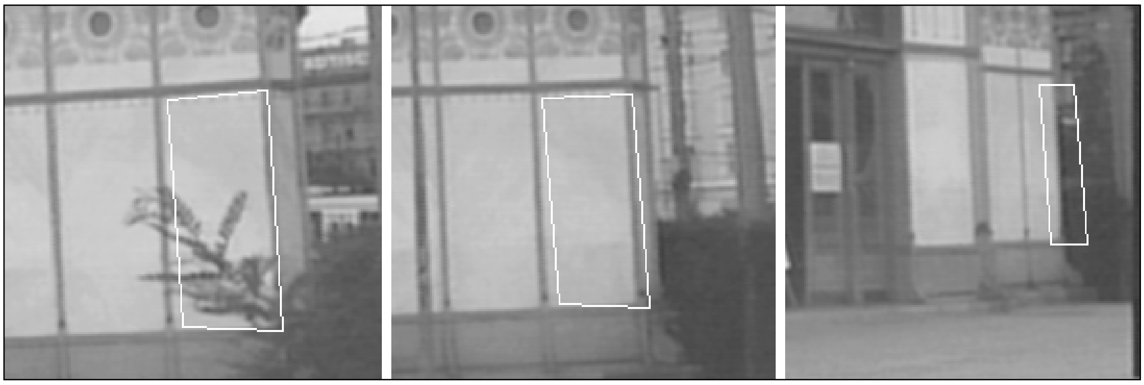

(b.) initial position of feature as from approximate model.

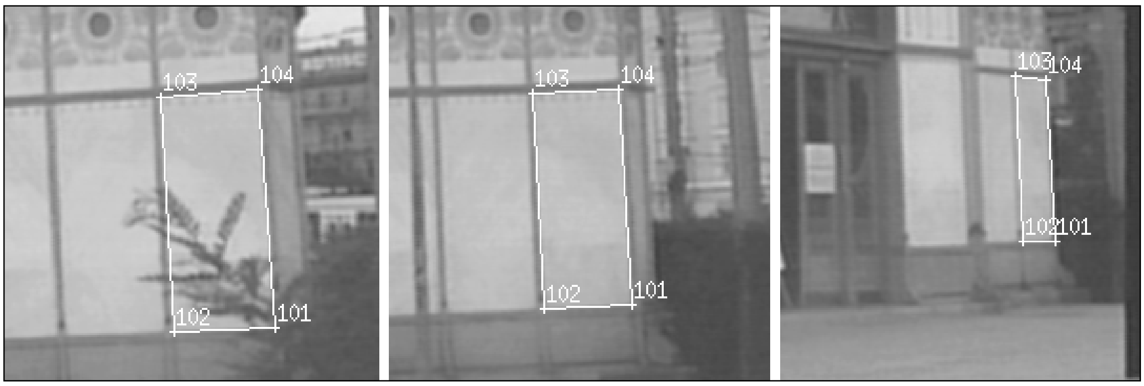

(c.) final position of feature after 5 iterations.

Figure 6: 3D-FEX.

The average precision of the object coordinates is used to analyse the results of positioning and are computed as:

$$\hat{\sigma}_X = \sqrt{\sum \hat{\sigma}^2_{X_i} / n_{Ob}}, \ \hat{\sigma}_Y = \sqrt{\sum \hat{\sigma}^2_{Y_i} / n_{Ob}}, \ \hat{\sigma}_Z = \sqrt{\sum \hat{\sigma}^2_{Z_i} / n_{Ob}} \quad \text{(Eq. 15)}$$

with n_{Ob} as the number of object points.

These calculations are necessary to make reliable statements about the estimated results (the object) as well as to judge whether the constraints of the knowledge-base are fulfilled or not. Figure 6 gives an example of the performance of this iterative procedure with a spatial intersection of a single feature in three images simultaneously.

5. PRACTICAL EXAMPLE

The architectural object is one of Otto Wagner's Stadtbahn Station buildings on the Karlsplatz in Vienna (see Figure 7). The dimensions of the building are 15 x 8 x 10 m^3. The described work was done as part of the contribution to the CIPA (International Committee for Architectural Photogrammetry) project "Karlsplatz". The idea and the initiative of this project belongs to P. Waldhäusl [18] and the aim was to check the current state-of-the-art in architectural photogrammetry. Therefore a small test object has been selected, photographed, measured and documented, in order to have well-checked materials to train students and photogrammetrists as well as to evaluate internationally the results of the analytic photogrammetric process with various cameras, with different software and with different kinds and amount of control information.

Figure 7: "O. Wagner Pavillion", Karlsplatz, Vienna.

Figure 8: Camcorder JVC GR-S77E.

In this test the image acquisition was performed with an inexpensive S-VHS camcorder. Although camcorders are not intended for photogrammetric use, they exhibit many useful characteristics. They are inexpensive and widely used for other purposes as well, they are portable and free-hand, they need no special equipment, they offer the ability of on-site quality control. Furthermore they provide very inexpensively means for storage of huge amount of video data in video tapes. The imaging system JVC Camcorder GR-S77E (see Figure 8) incorporates a 1/2" color sensor (6.4x4.8 mm^2). The analog images are stored on a S-VHS video tape and have to be digitized by a framegrabber. The digitized images have a size of 728x568 pixel. Accuracies exceeding 0.05 of the pixel spacing and a relative accuracy of 1:15000 in object space can be obtained with this sensor under laboratory conditions [19].

The photogrammetric analysis of the digital image data was performed with DIPAD. The image acquisition took place in a way that an image sequence from the object was generated by a person walking with the camera around the object and filming all four facades.

From this video tape 38 single frames were randomly digitized with a framegrabber. The mean distance between the camera and the object was about 16 m, which results in an image scale of 1:1800. The image analysis was performed with a bundle adjustment. All camera parameters and object coordinates were unknown. Totally 1611 object coordinates were determined to describe the entire building. Therefore 2589 image points have been measure semi-automatically by the 3D-FEX routine. The normal equation system which has to be solved consists of 5178 observations and 1726 unknowns. The precision of the object coordinates was determined as a part of the bundle adjustment routine. The results indicate a precision in object space (cf. Eq. 15) of 1.1 cm in X, 1.3 cm in Y, and 0.7 cm in Z, with X- and Y-axis in plane and Z-axis in height. This corresponds to 6.7 µm in image space. A more detailed description of the numerical results of this test is given in [20]. Different representations of the photogrammetrically derived CAD-model are shown in Figure 9.

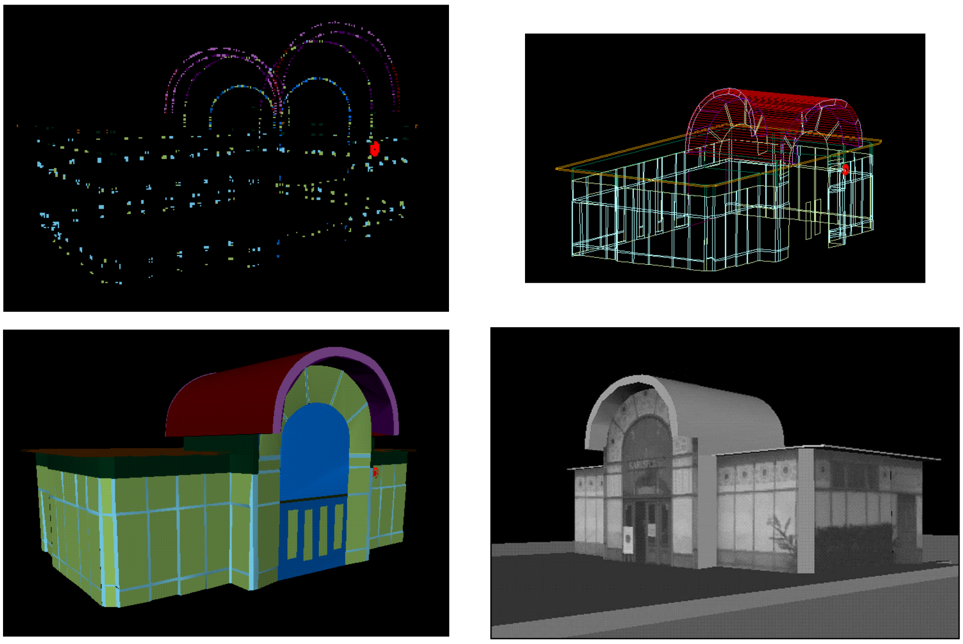

Figure 9: Photogrammetrically generated CAD-Model of test object.
upper left: point model
upper right: wireframe model
lower left: surface model
lower right: surface model draped with original image data

6. CONCLUSIONS

In this paper we described the current and planned functionality of DIPAD which brings together the functionality of CAAD and state-of-the-art photogrammetric computer measurement procedures. Pointing out briefly the many possible applications of digital photogrammetry in CAAD related fields as well as the main ideas and aspirations of the project, the main focus of the paper was the current integration of the CAAD and the photogrammetric system and the caad-based 3D feature extraction. The data-integration is achieved using a knowledge-base. On top of an adequate data-transfer between the two systems this knowledge-base enables constraint-based modelling in CAAD and qualitatively controlled measurement in DIPS. DIPAD allows the efficient and precise “as-built” modelling of architectural objects and holds a promise for a more widespread application of photogrammetry in the architectural field.

7. REFERENCES

[1] Fellbaum, M., “Low cost systems in architectural photogrammetry”, Int. Arch. Photogramm. and Remote Sensing, Washington DC, Vol 29, Part B5, 1992, pp. 771 - 777.

[2] Schenk, T., “Digital photogrammetric stations”, Proceedings of 2nd Course in Digital Photogrammetry, University of Bonn, Feb. 1995.

[3] Luhmann, T., “Bilderfassung in der Nahbereichsphotogrammetrie - Aktuelle Tendenzen”, Vermessungswesen und Raumordnung (VR 54/8), Wichmann-Verlag Karlsruhe, 1992, pp. 400-410.

[4] Shortis, W.R., Snow, W.L., Goad, W.K., “Comparative tests of industrial and scientific CCD cameras using plumb line and test range calibrations”, International Archives of Photogrammetry and Remote Sensing, Vol. 30, Part 5W1, 1995, pp. 53-59.

[5] Uttal, W. R., “On Seeing Forms”, Hillsdale, NJ, LEA Publishers, 1988.

[6] Nalwa, V. S., “Computer Vision”, Addison Wesley Publishing Company, 1993.

[7] Venturi, R., “Complexity and Contradiction in Architecture”, Museum of Modern Art, 1966.

[8] Slutzky, R., Rowe, C. , Hösli B. (Editor), “Transparenz”, Birkhaeuser Verlag, 1974.

[9] Mitchell, W. J., “The Logic of Architecture. Design, Computation, and Cognition”, Cambridge, MA, MIT Press, 1990.

[10] Rudolph, D., Stürznickel, T., Weissenberger, L., “Der DXF-Standard”, Rossipaul Verlag (Edition Autodesk), Mnchen, 1993.

[11] Coyne, R.D., Rosenman, M.A., Radford, A.D., Balachandran, M., Gero, J.S., “Knowledge-Based Design Systems”, Addison Wesley Publishing Company Inc, Reading, Mass., 1990.

[12] Hirschberg, U., Streilein, A. “CAAD meets Digital Photogrammetry - modelling weak forms for computer measurement”, Proceedings of ACADIA’95, Seattle, October 18-20, 1995, In press.

[13] Karara, H.M. (Editor), “Non-Topographic Photogrammetry”, Second Edition, American Society of Photogrammetry and Remote Sensing, Falls Church, Virginia, 1995.

[14] Brown, D.C., “A solution to the general problem of multi station analytical stereo-triangulation”, RCA Technical Report No. 43, 1958.

[15] Schmid, H., “Eine allgemeine analytische Lösung für die Aufgabe der Photogrammetrie”, Bildmessung und Luftbildwesen, 4/1958, pp. 103-112.

[16] Brown, D.C., “Close-Range Camera Calibration”, Photogrammetric Engineering, 37(8), 1971, pp. 855-866.

[17] Beyer, H., “Geometric and Radiometric Analysis of a CCD-camera-based photogrammetric close-range system”, Dissertation No. 9701, ETH-Zurich, 1992.

[18] Waldhäusl, P., “A test object for architectural photogrammetry: Otto Wagners underground station Karlsplatz in Vienna”, Proceedings of the XIV. International Symposium of CIPA, October 2-5, 1991, Delphi, Greece, pp. 247-251.

[19] Beyer, H., Kersten, T., Streilein, A., “Metric Accuracy Performance of Solid-State Camera Systems”. Paper presented at the SPIE OE/Technology’92 - Videometrics conference, 15-20 November 1992, Boston, MA. Published in SPIE Vol. 1820, Videometrics, pp. 103-110.

[20] Streilein, A. “Videogrammetry and CAAD for architectural restitution”, Proceedings of the Third conference on Optical 3-D Measurement Techniques, October 2-4, 1995, Vienna, Austria, in press.